electronic reprint

Acta Crystallographica Section B
Structural Science
ISSN 0108-7681

The commensurate composite σ-structure of β-tantalum

Alla Arakcheeva, Gervais Chapuis, Henrik Birkedal, Phil Pattison and Vladimir Grinevitch

Acta Crystallographica Section B
Structural Science
ISSN 0108-7681

The commensurate composite σ-structure of β-tantalum

Alla Arakcheeva,[a,b] Gervais Chapuis,[a]* Henrik Birkedal,[a] Phil Pattison[a] and Vladimir Grinevitch[b]

[a]Institute of Crystallography, University of Lausanne, BSP, 1015 Lausanne, Switzerland, and [b]Baikov Institute of Metallurgy, RAS, 119991 Moscow, Russia

Correspondence e-mail: gervais.chapuis@ic.unil.ch

Received 20 December 2002
Accepted 22 April 2003

The single-crystal investigation of the self-hosting σ-structure of β-tantalum (β-Ta) at 120 K (low-temperature, LT, structure) and at 293 K (RT-I before cooling and RT-II after cooling and rewarming; RT represents room temperature) shows that this structure is indeed a specific two-component composite where the components have the same (or an integer multiple) lattice constants but different space groups. The space groups of both host (H) and guest (G) components cause systematic absences, which result from their intersection. The highest symmetry of a σ-structure can be described as [H: $P4_2/mnm$; G: $P4/mbm$ ($c_G = 0.5c_H$); composite: $P4_2/mnm$]. A complete analysis of possible symmetries is presented in the *Appendix*. In β-Ta, two components modify their symmetry during the thermal process 293 K (RT-I) $\Rightarrow$ 120 K (LT) $\Rightarrow$ 293 K (RT-II): [H: $P\bar{4}2_1m$; G: $P\bar{4}2_1m$; composite: $P\bar{4}2_1m$] $\Rightarrow$ [H: $P\bar{4}$, G: $P4/mbm$ ($c_G = 0.5c_H$), composite: $P\bar{4}$] $\Rightarrow$ [H: $P\bar{4}2_1m$, G: $P4/mbm$ ($c_G = 0.5c_H$), composite: $P\bar{4}2_1m$]. Thus, the phase transition is reversible with respect to H and irreversible with respect to G.

1. Introduction

As was previously reported by Moseley & Seabrook (1973, and references cited therein), tetragonal β-tantalum (β-Ta) is a non-equilibrium phase in the pressure–temperature diagram. It crystallizes in the σ-phase structure type (Frank & Kasper, 1958, 1959) which is similar to the high-temperature β-U phase. Single-crystal X-ray structure investigation results confirm the structure type for β-Ta at room temperature (Arakcheeva *et al.*, 2002; hereafter referred to as the room-temperature RT-I β-Ta structure).

A σ-phase structure was detected for the Fe–Cr alloy in space group $P4_2/mnm$ by Bergman & Shoemaker (1954). Later, this complex tetragonal structure, very common for binary intermetallic compounds in some systems such as Cr–Fe, V–Ni, Nb–Re, Cr–Co and others, was always described in this space group (Frank & Kasper, 1958, 1959; Pearson, 1972). A schematic representation of a σ-phase structure is shown in Fig. 1 in a projection along the 4_2 axis. Two primary hexagonal-triangular Kagome nets $3636 + 3^26^2 + 6^3$(3:2:1) are located in mirror planes m_N normal to the 4_2 axis at $z = 1/4$ (black spheres in Fig. 1) and 3/4 (white spheres in Fig. 1); two secondary nets 3^2434 lie between the primary ones at $z = 0$ and 1/2 (grey spheres in Fig. 1; notation from Pearson, 1972).

The first doubt concerning the space group of a σ phase appeared when Donohue & Einspahr (1971) tried to refine the structure of β-U on the basis of X-ray powder diffraction data. Three space groups, $P4_2nm$, $P\bar{4}n2$ and $P4_2/mnm$, are listed by Donohue (1974) for β-U. The results of the corresponding refinements were characterized by both high values for the R

factors (more than 20%) and some interatomic distances which were too short. Later, neutron powder diffraction data (Lawson *et al.*, 1988) confirmed the space group $P4_2/mnm$ for β-U. Only the subgroup $P\bar{4}2_1m$ could correctly describe the RT-I β-Ta structure determined by single-crystal X-ray study. The σ-phase structure allows some space-group variations owing mainly to small atomic deviations from the mirror planes. Up to now, this possibility has been observed only for β-Ta. The long story of space-group determination for β-U (Donohue & Einspahr, 1971; Donohue, 1974; Lawson *et al.*, 1988, and references cited therein) shows that it is very difficult to determine these atomic deviations from powder diffraction data. However, according to the currently available information (ICSD), there is no single-crystal structure investigation of any σ phase, except the RT-I β-Ta structure, despite many metallic alloys crystallizing in this structure type (Pearson, 1972).

The interest of the σ-type structures, in particular, their symmetries, is reinforced owing to the close relationship between the σ-phase structures and the complex tetragonal structures of the high-pressure (HP) phases which have been intensively studied recently for the elements Rb (Schwarz *et al.*, 1999, McMahon *et al.*, 2001), Ba (Nelmes *et al.*, 1999), Bi, Sr, Sb and As (McMahon *et al.*, 2000). As previously shown (Arakcheeva *et al.*, 2002, and references cited therein), the

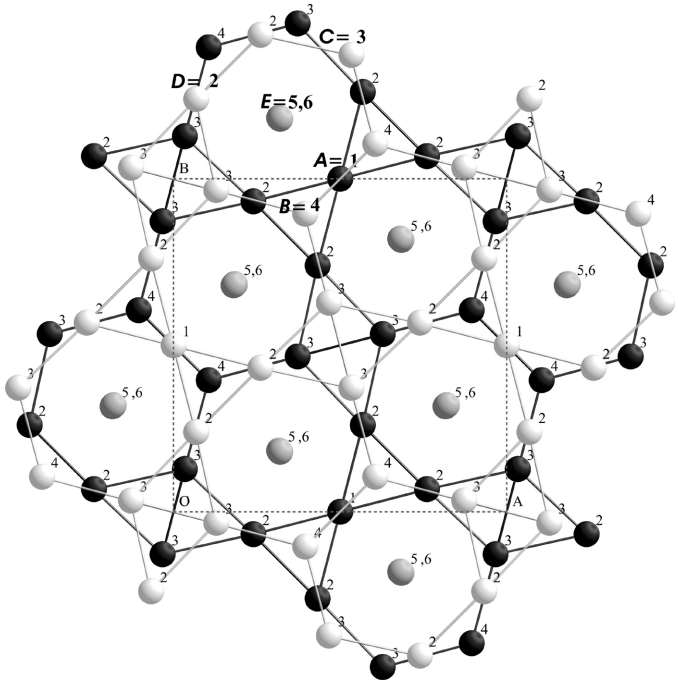

Figure 1
The (001) projection of a tetragonal σ-structure. The A, B, C and D atoms form the primary Kagome nets $3636 + 3^26^2 + 6^3$(3:2:1) of the host component. The E atoms form the secondary nets 3^2434 of the guest component. The primary nets are located in the mirror plane m_N of the highest symmetry space group $P4_2/mnm$ that is possible for the structure; z = 0.25 (black spheres) and 0.75 (white spheres). The secondary nets (grey spheres) are located in the levels $z \simeq 0$ and 0.5. The highest possible space group is $P4/mbm$ ($c_G = 0.5c_H$) for the guest component.

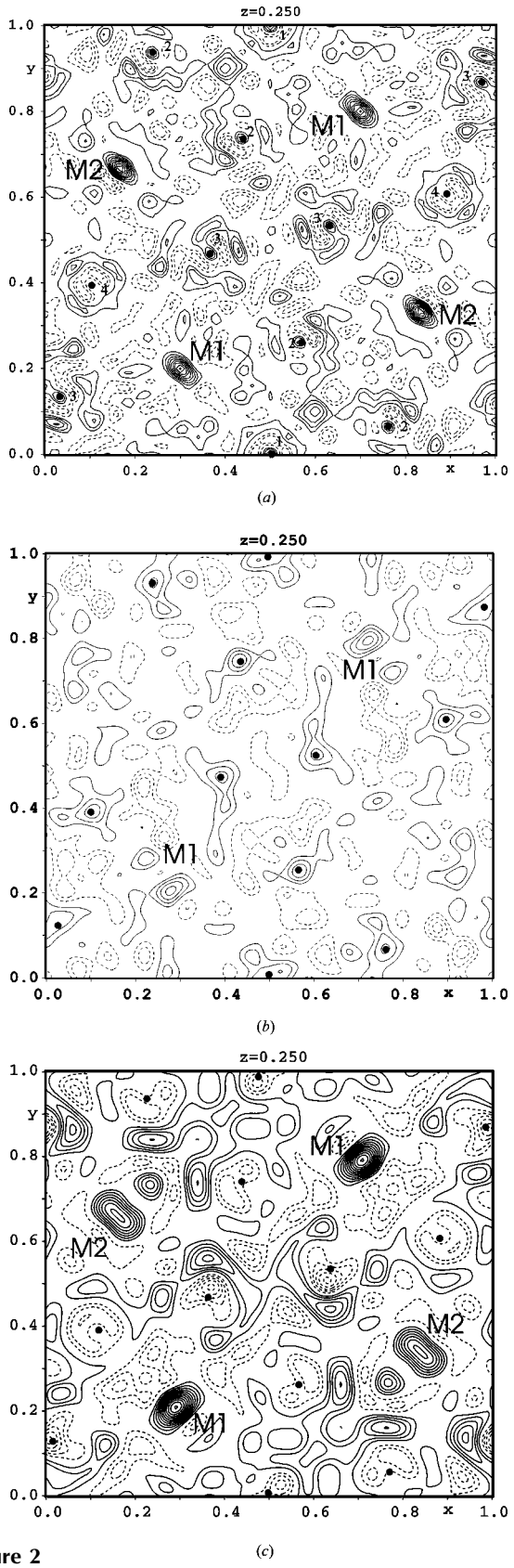

Figure 2
Residual electron-density sections calculated for β-Ta: (*a*) RT-I structure, (*b*) LT structure and (*c*) RT-II structure. *M*1 and *M*2 indicate the highest maxima. The black circles and numbers in (*a*) indicate the position of the Ta atoms. The increment between the lines is 2 e Å^{-3}. Solid and dashed lines indicate positive and negative electron density, respectively.

composite host–guest character is the main common feature of all these structures including the σ phase. In a σ-phase structure (Fig. 1), two primary Kagome nets form the host (H) substructure and two secondary nets form the guest (G) substructure with G atoms occupying channels formed in the framework of the H-component. In the HP phases, similar to the σ-phase structure, the atoms of the G-component are located in channels of the H-component which is formed by two nets connected by a 4_2 axis (for a comparative representation, see Arakcheeva *et al.*, 2002, Fig. 2). In the HP phases, the difference between the symmetries and the lattice constants of the H and the G components increases with pressure leading eventually to an incommensurate modulation.

No satellite reflections and/or any different lattice constant confirming a modulation were observed for a single crystal of β-Ta at room temperature measured with a CCD detector. In the present study, we pursue our structure investigation of β-Ta at low temperature. The composite host–guest character of the β-Ta structure and its specific features have been analysed using single-crystal synchrotron diffraction data obtained at 120 K (LT structure) and compared with two room-temperature structures: the previously determined RT-I structure obtained before cooling and an RT-II structure obtained from X-ray single-crystal diffraction data after cooling and rewarming.

2. Experimental

The electrolytic synthesis of β-Ta single crystals has been described in detail (Arakcheeva *et al.*, 2002). In the present investigation, the same single crystal has been used for the synchrotron diffraction experiment at 120 K and for the room-temperature X-ray measurements obtained after cooling and rewarming. As in our previous study, the irregular isometric crystal (minimum, average and maximum sizes are 0.018, 0.020 and 0.022 mm, respectively) was approximated by a sphere (r = 0.02 mm) for the absorption correction of the intensities (μ = 148.96 cm^{-1} for λ = 0.700013 Å of synchrotron radiation and μ = 147.48 cm^{-1} for Mo $K\alpha$ X-ray).

2.1. Diffraction study of β-Ta at 120 K (LT structure)

Synchrotron radiation single-crystal diffraction data were collected on a 20 µm crystal at the Swiss–Norwegian Beam Line (ESRF, France) at 120 (2) K. A wavelength of λ = 0.70013 Å was selected using a Si(111) double-crystal monochromator with a bent single crystal for sagittal focusing. Rh-coated mirrors were used for additional focusing and harmonic rejection. Data were collected using a MAR345 imaging plate system with a crystal-to-detector distance of 95 mm. A total of 180 frames were measured in the oscillation mode employing a 2° oscillation range. Data reduction was performed using *DENZO* and *SCALEPACK* of the *HKL* package (Otwinowski & Minor, 1997). The degree of linear polarization was assumed to be 0.96, in agreement with values previously determined for the present experimental configuration (Birkedal, 2000). Only repeated measurements of reflections with the same indices were used for scaling (which corrects for decay of the incident beam intensity); no assumptions were made about the crystal symmetry.

The tetragonal unit-cell parameters for the LT structure [a = 10.1815 (5), c = 5.2950 (1) Å; V = 548.90 (4) Å^3] were refined using the 6853 reflections with $I > 3\sigma(I)$ of the 8379 reflections [$3.79 < \theta < 30.52°$; $-14 < h < 14$, $-14 < k < 14$, $-7 < l < 7$]. No satellite reflections were observed. As in the RT-I data collection, the observation of reflections {001}, {003} and {005} with $I > 5\sigma(I)$ excluded the 4_2 axis and 79 reflections {0kl} with $I > 3$–$10\sigma(I)$ excluded the n-plane, the space group $P4_2/mnm$ and its subgroups containing the same glide plane, respectively. In addition, reflections {300}, {500}, {700}, {900} and {13.00} with $I > 3\sigma(I)$ excluded the 2_1 axis. The only space group for the LT phase compatible with these absences is $P\bar{4}$, a subgroup of $P\bar{4}2_1m$ characteristic of the RT-I structure. Averaging of the equivalent measurements (R_{av} = 0.0816) was performed for the non-centrosymmetric point group $\bar{4}$ (the Fridel pairs were not averaged).

Since the diffraction data point to a change of the β-Ta symmetry under cooling, a reinvestigation of the structure at room temperature has been performed in order to detect the reversibility of the phase transition.

2.2. Diffraction study of β-Ta at room temperature after cooling and rewarming (RT-II structure)

The KM-4 diffractometer (Mo $K\alpha$ radiation; tube voltage 55 kV; filament current 45 mA; KM-4 CCD/SAPPHIRE detector, sample–detector distance 61.4 mm, 630 frames) was used for the data collection [2912 reflections with $I > 3\sigma(I)$ in a quarter of reciprocal space; $3.84 < \theta < 28.06°$]. The tetragonal unit-cell parameters [a = 10.2010 (10), c = 5.3075 (5) Å] were refined from 2912 reflections with $I > 3\sigma(I)$. Similar to the RT-I experimental data, the only systematic extinction (h00, $h \neq 2n$) led to the space group $P\bar{4}2_1m$ for the RT-II structure. After absorption correction, the intensities averaged in point group $4mm$ (R_{av} = 0.0923) and $474F > 3\sigma(F)$ were used for the structure refinement.

3. Structure refinement

The *JANA*2000 program package (Petricek & Dusek, 2001) was used for all the structure calculations. The full-matrix refinements based on F with both isotropic and anisotropic atomic displacements were performed with the weighting scheme $w = 1/[\sigma^2(F) + 0.0001F^2]$. The extinction coefficients were obtained from the Becker–Coppens (B-C) type 1 Gaussian isotropic approximation (Petricek & Dusek, 2001).

3.1. Refinement of the LT β-Ta structure

There are 1530 independent intensities [$F > 3\sigma(F)$ averaged in point group $\bar{4}$] which have been used for the LT structure calculations. Taking into account the symmetry lowering from the space group $P\bar{4}2_1m$ at room temperature to $P\bar{4}$ at 120 K, the twin components connected by a mirror plane have been

Table 1
Experimental table.

	I	II
Crystal data		
Chemical formula	Ta_{30}	Ta_{30}
M_r	5428.4	5428.4
Cell setting, space group	Tetragonal, $P\bar{4}2_1m$	Tetragonal, $P\bar{4}$
a, c (Å)	10.2010 (10), 5.3075 (5)	10.1815 (5), 5.2950 (1)
V (Å^3)	552.3 (9)	548.9 (4)
Z	1	1
D_x (Mg m^{-3})	16.316 (3)	16.417 (1)
Radiation type	Mo $K\alpha$	Synchrotron
No. of reflections for cell parameters	2912	8379
θ range (°)	28.1	3.8–30.5
μ (mm^{-1})	147.75	148.66
Temperature (K)	293	120 (2)
Crystal form, colour	Isometric irregular, silver	Isometric irregular, silver
Crystal size (mm)	0.02 × 0.02 × 0.02	0.02 × 0.02 × 0.02
Data collection		
Diffractometer	Oxford Instruments KM4	MAR345
Data collection method	CCD scan	φ scans
Absorption correction	Sphere	For a sphere
T_{min}	0.028	0.024
T_{max}	0.050	0.049
No. of measured, independent and observed reflections	5271, 683, 474	8379, 1708, 1530
Criterion for observed reflections	$I > 3\sigma(I)$	$I > 3\sigma(I)$
R_{int}	0.092	0.082
θ_{max} (°)	28.1	30.5
Range of h, k, l	$-13 \Rightarrow h \Rightarrow 13$ $-11 \Rightarrow k \Rightarrow 13$ $-6 \Rightarrow l \Rightarrow 6$	$-14 \Rightarrow h \Rightarrow 14$ $-14 \Rightarrow k \Rightarrow 14$ $-7 \Rightarrow l \Rightarrow 7$
Refinement		
Refinement on	F	F
$R[F^2 > 2\sigma(F^2)]$, $wR(F^2)$, S	0.058, 0.040, 3.93	0.036, 0.050, 1.74
No. of relections	474	1530
No. of parameters	24	72
H-atom treatment	No H atoms present	No H atoms present
Weighting scheme	Based on measured s.u.'s $w = 1/\sigma^2(F)$	Based on measured s.u.'s $w = 1/[\sigma^2(F) + 0.0001F^2]$
$(\Delta/\sigma)_{max}$	0.001	0.001
$\Delta\rho_{max}$, $\Delta\rho_{min}$ (e Å^{-3})	24.22, −11.35	11.04, −9.89
Extinction method	B–C type 1 Gaussian isotropic (Becker & Coppens, 1974)	C type 1 Gaussian isotropic (Becker & Coppens, 1974)
Extinction coefficient	0.000648	0.0009 (3)

Computer programs: *JANA*2000 (Petricek & Dusek, 2001).

accounted for in the computation using the matrix (010/100/00−1). The coefficients of the twin components never deviated from 1/2 by more than a standard deviation.

3.1.1. Refinement in space group $P\bar{4}$. Following the systematic extinctions, the refinement of the structure in space group $P\bar{4}$ was based on the atomic sites of the RT-I structure from the refinement in space group $P\bar{4}2_1m$. The coordinates of the Ta1 atom located on the twofold axis and the coordinates of the Ta4, Ta5 and Ta6 atoms located on the diagonal mirror plane were taken without change; the general positions Ta2 and Ta3 were split (Ta2*a*, Ta2*b* and Ta3*a*, Ta3*b*) by the *m* plane. According to the self-hosting structure description of β-Ta (Arakcheeva *et al.*, 2002), atoms Ta1, Ta2*a*, Ta2*b*, Ta3*a*, Ta3*b* and Ta4 form two primary Kagome nets of the host component (H), while atoms Ta5 and Ta6 form two secondary nets of the guest component (G) (Fig. 1). Refinement with isotropic atomic displacements lead to $R = 0.0393$ [$wR = 0.0633$; GOF = 2.01; the reflections-to-parameters ratio (r/p) was equal to 43.3; $\Delta\rho_{\mu\alpha\xi} = 15.3$ e Å^{-3}, $\Delta\rho_{min} = -10.3$ e Å^{-3}]. Anisotropic atomic displacements yielded $R = 0.0355$ [$wR = 0.0474$; GOF = 1.65; $r/p = 21.55$; extinction coefficient 0.0009 (3); $\Delta\rho_{max} = 11.4$ e Å^{-3}; $\Delta\rho_{min} = -9.53$ e Å^{-3}]. Experimental details are given in Table 1.[1] The atomic parameters obtained for LT β-Ta in space group $P\bar{4}$ are listed in Table 2. The alphabetic notation of the atoms is used here according to Frank & Kasper (1959) in the σ-structure.

3.1.2. Composite character of the β-Ta σ-structure. Analysis of the atomic coordinates resulting from the refinement of the LT structure in the space group $P\bar{4}$ shows that the deviations from their positions relative to the supergroup $P4_2/mnm$ (which is the highest for a σ-phase structure) are very small.

In space group $P4_2/mnm$, the following relations are valid, taking into account a shift (0.5, 0, −0.25) of the origin which was used for this space group in order to refer to the atomic coordinates listed in Table 2:

(i) For Ta1–Ta4 atoms, $z = 0.25$ owing to their location on the mirror plane (m_N) normal to the 4_2 axis. The Ta1 atom (indicated as *A*) refers to the position 2*a*(0,0,0) in the standard setting.

(ii) y(Ta4) = −[0.5 + x(Ta4)], as Ta4 is located on the diagonal mirror plane (m_D); Ta4 (indicated as *B*) refers to position 4*g*:(x,−x,0) in the standard setting;

(iii) x(Ta2*b*) = 0.5 − y(Ta2*a*), y(Ta2*b*) = 0.5 − x(Ta2*a*), as Ta2*a* and Ta2*b* are connected by the m_D-plane resulting in one Ta2 position (indicated as *D*). The same relations are valid for Ta3*a* and Ta3*b* (indicated as *C*). Both Ta2 and Ta3 refer to the position 8*i*(x,y,0) in the standard setting.

(iv) y(Ta5) = x(Ta5) − 0.5, y(Ta6) = x(Ta6) − 0.5 as Ta5 and Ta6 are located on the m_D plane.

(v) z(Ta6) = 0.5 − z(Ta5), x(Ta6) = x(Ta5), y(Ta6) = y(Ta5) as Ta5 is connected to Ta6 by the m_N plane which is located in $z = 0.25$ in the standard setting of the space group. Atoms Ta5 and Ta6 together form the position 8*j*(x,x,z) (indicated as *E*) in the standard setting.

[1] Supplementary data for this paper are available from the IUCr electronic archives (Reference: SN0032). Services for accessing these data are described at the back of the journal.

Table 2
Atomic parameters of β-Ta (LT1 structure; T = 120 K) obtained with the space group $P\bar{4}$.

Atom	Notation	Position	x	y	z	$U_{eq} \times 10^2$ (Å^2)
Ta1	*A*	2(*g*)	0.5	0	0.2473 (5)	0. 56 (3)
Ta2*a*	*D*	4(*h*)	0.75989 (11)	0.06588 (8)	0.2493 (3)	0.55 (3)
Ta2*b*	*D*	4(*h*)	0.43193 (8)	−0.26226 (11)	0.2518 (3)	0.56 (3)
Ta3*a*	*C*	4(*h*)	0.03415 (9)	0.12780 (10)	0.2520 (4)	0.57 (3)
Ta3*b*	*C*	4(*h*)	0.37046 (10)	−0.53529 (10)	0.2487 (4)	0.55 (4)
Ta4	*B*	4(*h*)	0.10648 (10)	−0.60485 (9)	0.2519 (3)	0.56 (3)
Ta5	*E*	4(*h*)	0.8180 (3)	0.3183 (3)	0.0005 (2)	0.56 (3)
Ta6	*E*	4(*h*)	0.8178 (3)	0.3183 (3)	0.5005 (2)	0.59 (3)

Note: (i) *A*, *B*, *C* and *D* atoms build up primary Kagome nets $3636 + 3^2 6^2 + 6^3(3{:}2{:}1)$ of the H component; *E* atoms build up secondary nets 3^2434 of the G component. (ii) Two *E* sites actually merge into one position $4g(x, x + 0.5, 0)$ of space group $P4/mbm$ ($c_G = 0.5c_H$) with x = 0.8179 (3).

Table 3
Atomic parameters of β -Ta (LT1; T = 120 K) obtained for the composite structure with the symmetry: H: $P\bar{4}$; G: $P4/mbm$ ($c_G = 05c_H$); composite structure: $P\bar{4}$.

Atom	Notation	Position	x	y	z	$U_{eq/iso^*} \times 10^2$ (Å^2)
Host component: space group $P\bar{4}$						
Ta1	*A*	2(*g*)	0.5	0	0.2548 (5)	0.54 (3)
Ta2*a*	*D*	4(*h*)	0.75963 (10)	0.06646 (7)	0.2493 (4)	0.55 (3)
Ta2*b*	*D*	4(*h*)	0.43251 (8)	−0.26252 (9)	0.2521 (5)	0.56 (3)
Ta3*a*	*C*	4(*h*)	0.03408 (9)	0.12735 (10)	0.2519 (5)	0.54 (3)
Ta3*b*	*C*	4(*h*)	0.37007 (9)	−0.53527 (9)	0.2488 (5)	0.57 (3)
Ta4	*B*	4(*h*)	0.10620 (9)	−0.60509 (9)	0.2513 (4)	0.56 (3)
Guest component: space group $P4/mbm$; $c_G = 0.5c_H$						
Ta5	*E*	4(*g*)	0.81809 (3)	x + 0.5	0 (0 and 0.5 in the H cell)	0.567 (15)

In space group $P4_2/mnm$ relations (i)–(iii) completely describe the two primary atomic nets of H (*A*, *B*, *C* and *D* atoms) located on two levels (z = 0.25 and 0.75) and which coincide with the mirror plane m_N (Fig. 1). The two secondary nets of G (*E* atom) located at z = 0 and 0.5 (halfway between the primary nets) are not only related to each other by the m_N planes [relation (v)], but also by the mirror planes m_N on which they are lying. They are not required by the space group $P4_2/mnm$. The mirror planes m_N of the secondary nets exist only for the G component but not for the H component. If in relation (v) z(Ta5) = 0, then z(Ta6) = 0.5, which means Ta5 is related to Ta6 by the translation $c_G = 0.5c_H$. Both positions form the $4g(x,x + 0.5,0)$ site of space group $P4/mbm$ ($c_G = 0.5c_H$). Therefore, for the highest symmetry available for the whole structure (space group $P4_2/mnm$), the symmetry of H (space group $P4_2/mnm$) is lower than the symmetry of G, which is the minimal non-isometric supergroup $P4/mbm$ with the lattice parameter c_G being half that of c_H. This conclusion concerning the difference of symmetry between the H and the G components is not only valid for β-Ta but for all σ-phase structures as well.

In the H substructure refinement of the LT structure model in space group $P\bar{4}$ (Table 2), it appears that the deviations of the atoms from their positions corresponding to space group $P4_2/mnm$ are small. A maximal atomic shift 0.014 (4) Å eliminates the m_N plane [relations (i)]; the maximal discrepancy of the atomic positions from the m_D planes is estimated as 0.020 (3) Å [relations (ii) and (iii)]. These deviations confirm and correspond to the weak experimental reflections ($h00, h = 2n + 1$; $00l, l = 2n + 1$; $0kl, k + l = 2n + 1$). However, no deviations of the atoms from the corresponding positions in space group $P4/mbm$ ($c_G = 0.5c_H$) can be observed in the G substructure (*E* atoms in Table 2). Relations (iv) and (v) with z(Ta5) = 0 [z(Ta6) = 0.5, respectively] support the highest available symmetry of G within one standard deviation (see footnote to Table 2).

Therefore, β-Ta exhibits a composite character at 120 K. The space group of G is $P4/mbm$ with the parameter $c_G = 0.5c_H$. This result of the structure refinement in space group $P\bar{4}$ leads us to consider all the possible combinations of G with H which together would not generate any systematic extinction.

We present in the *Appendix* the complete systematic analysis of all possible H + G combinations yielding a composite tetragonal σ-structure.

3.1.3. Selection of composite structure models for the LT structure. According to the results of the systematic analysis (see the *Appendix*), no composite structure model among 54 variants of the H + G combinations generates any systematic absence condition (in Table 9, see variants with *Abs*: none). Among them, the space group $P2_z11$ of the composite structure has the lowest symmetry. In this space group, the refinement of the structure converged to R = 0.0373 (wR = 0.0523, GOF = 1.86, anisotropic atomic displacements). Owing to the lower symmetry, both the H and the G atomic sets were split in comparison to the atomic positions described in §3.1.2: *A* = Ta1*a* + Ta1*b*; *B* = Ta4*a* + Ta4*b*; *C* = Ta3*aa* + Ta3*ab* + Ta3*ba* + Ta3*bb*; *D* = Ta2*aa* + Ta2*ab* + Ta2*ba* + Ta2*bb*; *E* = Ta5*a* + Ta5*b* + Ta6*a* + Ta6*b*. The differences between the atomic coordinates were less than one standard deviation for the atoms connected by the $\bar{4}$-fold axis. Following the results obtained earlier in $P\bar{4}$, four sites of *E* atoms (G substructure) were indeed merged into one position, $4g(x,x + 5,0)$, of space group $P4/mbm$ ($c_G = 0.5c_H$). As seen from Table 9, there is only one H + G combination which does not generate any systematic absence for the space group of the G component: H: $P\bar{4}$; G: $P4/mbm$ ($c_G = 0.5c_H$); composite structure: $P\bar{4}$. Thus, this unique model was chosen for the final refinement of the LT structure.

3.1.4. Refinement of the LT composite structure. In order to obtain the composite model, the refinement was performed in space group $P\bar{4}$ subject to the relations (iv) and (v) with z(Ta5) = 0 and z(Ta6) = 0.5. As expected, the characteristics of the refinement [R = 0.0363; wR = 0.0501; GOF = 1.74; r/p = 26.38; extinction coefficient 0.0009 (3); $\Delta\rho_{max}$ = 11.04 e Å^{-3}; $\Delta\rho_{min}$ = −9.89 e Å^{-3}] are almost equal to those obtained in

Table 4
Atomic parameters of β-Ta obtained with space group $P\bar{4}2_1m$ at room temperature before (RT-I) and after (RT-II) cooling and rewarming.

RT-I: a = 10.211 (3), c = 5.3064 (10) Å; RT-II: a = 10.2010 (10), c = 5.3075 (5) Å.

		x		y		z		$U_{eq} \times 10^2$ (Å^2)	
Atoms (Notation)	Position	RT-I	RT-II	RT-I	RT-II	RT-I	RT-II	RT-I	RT-II
Ta1 (*A*)	2(*g*)	0.5	0.5	0	0	0.228 (2)	0.244 (7)	1.3 (1)	0.48 (18)
Ta2 (*D*)	8(*f*)	0.7598 (3)	0.7610 (4)	0.0677 (3)	0.0674 (4)	0.235 (1)	0.246 (3)	1.52 (7)	0.51 (9)
Ta3 (C)	8(*f*)	0.0343 (3)	0.0342 (3)	0.1267 (4)	0.1286 (3)	0.255 (2)	0.243 (3)	2.9 (1)	0.43 (11)
Ta4 (*B*)	4(*e*)	0.1033 (4)	0.1042 (4)	−0.6033 (4)	−0.6042 (4)	0.235 (2)	0.240 (4)	2.79 (7)	0.42 (14)
Ta5 (*E*)	4(*e*)	0.8142 (6)	0.8189 (9)	0.3142 (6)	0.3189 (9)	0.003 (1)	0.002 (4)	2.0 (1)	0.3 (3)
Ta6 (*E*)	4(*e*)	0.8196 (5)	0.8185 (9)	0.3196 (5)	0.3185 (9)	0.491 (1)	0.500 (5)	1.9 (2)	1.0 (3)

Note: For the RT-II structure, two *E* sites actually merge into one position $4g(x, x + 0.5, 0)$ of space group $P4/mbm$ ($c_G = 0.5c_H$) with x = 0.8187 (9).

Table 5
Atomic parameters of the RT-II structure obtained with the space group $P112$ ($P2_z11$).

Atom	Notation	Position	x	y	z	$U_{iso} \times 10^2$ (Å^2)
Ta1*a*	*A*	1(*b*)	0.5	0.0	0.244 (3)	0.65 (13)
Ta1*b*	*A*	1(*c*)	0.0	−0.5	−0.244 (7)	0.69 (12)
Ta2*a*	*D*	2(*e*)	0.7611 (3)	0.0668 (5)	0.244 (6)	0.72 (9)
Ta2*b*	*D*	2(*e*)	0.0669 (4)	−0.7608 (4)	−0.243 (6)	0.79 (8)
Ta2*c*	*D*	2(*e*)	0.2606 (4)	0.4329 (5)	−0.244 (5)	0.79 (8)
Ta2*d*	*D*	2(*e*)	0.5673 (4)	0.2613 (4)	0.246 (6)	0.72 (8)
Ta3*a*	*C*	2(*e*)	0.0350 (4)	0.1287 (4)	0.245 (6)	0.79 (9)
Ta3*b*	*C*	2(*e*)	0.1291 (4)	−0.0342 (4)	−0.244 (6)	0.73 (9)
Ta3*c*	*C*	2(*e*)	0.5344 (4)	0.3715 (4)	−0.241 (6)	0.78 (9)
Ta3*d*	*C*	2(*e*)	0.6285 (4)	0.5350 (5)	0.246 (7)	0.93 (9)
Ta4*a*	*B*	2(*e*)	0.1045 (3)	−0.6047 (4)	0.242 (5)	0.68 (10)
Ta4*b*	*B*	2(*e*)	−0.6041 (4)	−0.1042 (4)	−0.240 (6)	0.71 (10)
Ta5*a*	*E*	2(*e*)	0.8187 (16)	0.3202 (19)	0.003 (6)	0.7 (4)
Ta5*b*	*E*	2(*e*)	0.3174 (15)	−0.8208 (18)	0.001 (6)	0.6 (4)
Ta6*a*	*E*	2(*e*)	0.8185 (17)	0.317 (2)	0.502 (6)	1.0 (4)
Ta6*b*	*E*	2(*e*)	0.3203 (17)	−0.817 (2)	−0.498 (6)	1.3 (4)

Note: (i) Four *E* sites (G component) actually merge into one position $4g(x, x + 0.5, 0)$ of space group $P4/mbm$ ($c_G = 0.5c_H$) with x = 0.8187 (18). (ii) Sites of the H component merge into the following positions of space group $P\bar{4}2_1m$ ($c = c_H$): two *A* sites: into one 2*g*(0.5,0,*z*), z = 0.244 (7); two *B* sites: into one 4*e*(*x*,*x* + 0.5,*z*), x = 0.1044 (4), z = 0.241 (6); four *C* sites: into one 8*f*(*x*,*y*,*z*), x = 0.0346 (4), y = 0.1289 (4), z = 0.244 (6); four *D* sites: into one 8*f*(*x*,*y*,*z*), x = 0.7609 (4), y = 0.0670 (4), z = 0.244 (6).

the space group $P\bar{4}$ without any symmetry restriction of the G component. The slightly increased R factors can be associated with the number of parameters which reduces from 71 to 58. The characteristics of the composite model of the LT structure are listed in Table 3.

3.2. Refinement of the RT-II β-Ta structure

After averaging 474 $F > 3\sigma(F)$ structural amplitudes ($-9 \le h \le 9$, $0 \le k \le 13$, $0 \le l \le 6$; $|h| \le k$) have been used for the refinement of the RT-II structure corresponding to the β-Ta crystal after a cooling cycle. Experimental details are listed in Table 1.

3.2.1. Refinement in space group $P\bar{4}2_1m$. The systematic absences of the room-temperature structure after cooling and rewarming (RT-II) were identical to those before cooling, *i.e.* RT-I, $P\bar{4}2_1m$. Therefore, we first performed the refinement of RT-II in this space group. The main characteristics of the refinement including anisotropic atomic displacement: R = 0.0633; wR = 0.0394; GOF = 3.06; extinction coefficient 0.0018 (4); $\Delta\rho_{max}$ = 28.74 e Å^{-3}; $\Delta\rho_{min}$ = −15.46 e Å^{-3}. Atomic coordinates for the RT-I and RT-II structures are listed in Table 4.

3.2.2. Composite character of the RT-II structure: selection of the composite structure model. A comparison between RT-I and RT-II (Table 4) both refined in the same space group $P\bar{4}2_1m$ reveals some differences. In RT-II, similar to the LT structure, the atomic coordinates of the *E* atoms (G substructure) corresponding to the $4g(x, x + 0.5, 0)$ position of the space group $P4/mbm$ ($c_G = c_H$) fit within one standard deviation (see notice to Table 4), whereas a deviation of 0.048 (5) Å is observed for the m_N plane in RT-I. This property points to the composite character of RT-II.

According to the systematic analysis (see *Appendix*), 32 H + G variants of the composite structure generate the absence $h00$, $h \neq 2n$, which is observed for RT-II. The space group $P2_z11$ has the lowest order among the selected 32 variants. Refinement of RT-II in this space group converged to R = 0.0594 (wR = 0.0755, GOF = 3.73, isotropic atomic displacements). An attempt to refine this model with anisotropic atomic displacements led to negative eigenvalues at all the atomic positions. The atomic coordinates obtained with U_{iso} are listed in Table 5. Similar to the results obtained with the space group $P\bar{4}2_1m$ (Table 4), four sites of *E* atoms in $P2_z11$ (G substructure) merge into one position, $4g(x,x + 5,0)$ of the space group $P4/mbm$ ($c_G = 0.5c_H$). As follows from Table 9, there is only one H + G combination where G = $P4/mbm$ and which generates the systematic absence $h00$, $h \neq 2n$; the symmetry for the corresponding composite structure is: H: $P\bar{4}2_1m$; G: $P4/mbm$ ($c_G = 0.5c_H$); composite structure: $P\bar{4}2_1m$. This H + G combination is confirmed by the atomic coordinates of the H substructure: two sites for *A*, two sites for *B*, four sites for both *C* and *D* in the lower space group $P2_z11$ (Table 5) merge into higher symmetrical sets of the space group $P\bar{4}2_1m$. In this space group each site combination of *A*, *B*, *C* and *D* merges into one single

Table 6
Atomic parameters of β-Ta (RT-II structure) obtained for the composite structure with the symmetry: H: $P\bar{4}2_1m$; G: $P4/mbm$ ($c_G = 0.5c_H$); composite structure: $P\bar{4}2_1m$.

Atom	Notation	Position	x	y	z	$U_{eq/iso*} \times 10^2$ (Å^2)
Host component: space group $P\bar{4}2_1m$						
Ta1	*A*	2(*g*)	0.5	0	0.247 (7)	0.50 (17)
Ta2	*D*	8(*f*)	0.7611 (3)	0.0674 (4)	0.246 (3)	0.50 (9)
Ta3	*C*	8(*f*)	0.0343 (3)	0.1286 (3)	0.241 (4)	0.41 (12)
Ta4	*B*	4(*e*)	0.1043 (4)	−0.6043 (4)	0.246 (6)	0.46 (15)
Guest component: space group $P4/mbm$; $c_G = 0.5c_H$						
Ta5	*E*	4(*g*)	0.81862 (16)	$x + 0.5$	0 (0 and 0.5 in the H cell)	0.58 (5)

Table 7
Comparison of the residual electron density of β-Ta: RT-I (T = 293 K before cooling); LT (T = 120 K); RT-II (T = 293 K after cooling and rewarming).

	RT-I	LT	RT-II
$\Delta\rho_{max}$; $\Delta\rho_{min}$ (e Å^{-3})	19.99; −11.39	11.06; −9.89	24.24; −14.57
The highest maxima			
*M*1: $\Delta\rho$ (e Å^{-3})	19.99	11.06	24.24
Position	4*e*(x, 0.5 − x, z) of space group $P\bar{4}2_1m$	4*h*(x,y,z) of space group $P\bar{4}$	4*e*(x, 0.5 − x, z) of space group $P\bar{4}2_1m$
(x_1 y_1 z_1)	(0.301 0.199 0.25)	(0.289 0.211 0.25)	(0.291 0.209 0.25)
Minimal distance from the Ta atoms (Å)	1.38	1.39	1.39
*M*2: $\Delta\rho$ (e Å^{-3})	18.90	–	14.37
Position	4*e*(x, x + 0.5, z) of space group $P\bar{4}2_1m$	–	4*e*(x, x + 0.5, z) of space group $P\bar{4}2_1m$
(x_2 y_2 z_2)	(0.826 0.326 0.25)	–	(0.839 0.339 0.25)
Minimal distance from the Ta atoms (Å)	1.37	–	1.35
Other maxima: $\Delta\rho$ (e Å^{-3})	9–12	7.5–9	9–14
Minimal distance from the Ta atoms (Å)	0.5–0.7	0.04–0.21	0.42–0.74
After including *M*1 and *M*2 as the Ta_{int} atom in refinement with B = 1.0 Å^2			
$\Delta\rho_{max}$; $\Delta\rho_{min}$ (e Å^{-3})	11.8; −11.3	8.98; −10.14	14.23; −11.31
Content of Ta_{int} in the unit cell (atom)	0.08 (2)	0.06 (1)	0.12 (4)
Decreasing of R factor	From 0.0566 to 0.0560	From 0.0363 to 0.0361	From 0.0582 to 0.0565

site, as given in Table 4. This was the reason for refining RT-II as a composite structure using the selected H + G combination.

3.2.3. Refinement of the composite structure. The combination of the space groups characteristic of the composite structure was realised using the space group $P\bar{4}2_1m$ and relation (v) with z = 0 for Ta5 and z = 0.5 for Ta6. The refinement was performed with anisotropic atomic displacement parameters to R = 0.0582 (wR = 0.0408, GOF = 3.93, $\Delta\rho_{max}$ = 24.22 e Å^{-3}, $\Delta\rho_{min}$ = −11.32 e Å^{-3}). The final atomic parameters are listed in Table 6. Note that the corresponding atomic coordinates are independent of the choice of the space group within the limit of one standard deviation (*cf.* Tables 4, 5 and 6).

4. The main features of the residual electron density of the LT and RT-II structures in comparison to RT-I

The final atomic parameters obtained for both the LT and RT-II composite models were used for the residual electron density calculations. The most intriguing (x,y,1/4) section is shown in Fig. 2 for LT (*b*) and RT-II (*c*) in comparison with RT-I (*a*). The comparative characteristics of the residual electron density for the three investigated β-Ta structures are shown in Table 7.

Evidently, $\Delta\rho_{max}$ depends on the accuracy of the experimental data and the quality of the refinement; the lowest value of $\Delta\rho_{max}$ = 11.06 e Å^{-3} correlates with the lowest R = 0.0363 which is characteristic of LT (synchrotron radiation experiment); the highest $\Delta\rho_{max}$ = 24.24 e Å^{-3} and R = 0.0582 correspond to RT-II. The slightly higher R factor obtained for RT-II compared with RT-I (R = 0.0566, $\Delta\rho_{max}$ = 19.99 e Å^{-3}) is a consequence of the crystal quality subject to the cooling cycle.

The positions of the two highest maxima (*M*1 and *M*2 in Fig. 2 and in Table 7) are the same for the RT-I and RT-II structures (within one standard deviation which is 0.009 for x and y, and 0.04 for z). In LT *M*1 is identical to *M*1 in RT-I and RT-II, however, *M*2 is absent in LT (Fig. 2).

The lower maxima of the residual electron density are located in the vicinity of the atomic positions but closer to the atoms at lower temperature (0.04–0.21 Å in LT) in comparison to the room-temperature structures (0.5–0.7 Å in RT-I and 0.4–0.7 Å in RT-II). These maxima seem to be connected with anharmonic temperature vibrations of the Ta atoms.

As we assumed earlier for the RT-I structure, the *M*1 and *M*2 maxima might be interpreted as additional Ta_{int} atoms intercalated in the G substructure with Ta_{int} − Ta5 (and Ta_{int} − Ta6) $\simeq$ 1.4 Å distances which are too short. Similar to RT-I, the *M*1 position in LT and both the *M*1 and *M*2 positions in RT-II included in the refinement as Ta_{int} fit the highest

Table 8
Structural characteristics of the composite β-Ta structure at T = 120 K (LT) and at T = 293 K before (RT-I) and after (RT-II) cooling.

Distances (Å)	RT-I structure; a = 10.211 (3), c = 5.3064 (10); c/a = 0.5197 Symmetry: H: $P\bar{4}2_1m$; G: $P\bar{4}2_1m$; composite structure: $P\bar{4}2_1m$	LT structure; a = 10.1815 (5), c = 5.2950 (1); c/a = 0.5201 Symmetry: H: $P\bar{4}$; G: $P4/mbm$; composite structure: $P\bar{4}$	RT-II structure; a = 10.2010 (10), c = 5.3075 (5); c/a = 0.5203 Symmetry: H: $P\bar{4}2_1m$; G: $P4/mbm$; composite structure: $P\bar{4}2_1m$
Host component (H)			
Ta—Ta in a net:			
Range	2.681 (7)–2.893 (7); Δ = 0.212	2.684 (1)–2.882 (1); Δ = 0.198	2.715 (5)–2.891 (5); Δ = 0.176
Average	⟨2.781⟩	⟨2.790⟩	⟨2.793⟩
Unusual	2.983 (8) for Ta4—Ta4	3.042 (1) for Ta4—Ta4	3.010 (5) for Ta4—Ta4
Ta—Ta between nets:			
Range	2.865 (7)–3.301 (7); Δ = 0.436	2.877 (2)–3.291 (3); Δ = 0.414	2.843 (2)–3.349 (2); Δ = 0.506
Average	⟨3.131⟩	⟨3.119⟩	⟨3.114⟩
Distances between average planes of nets	2.53 (2), 2.78 (2); Δ = 0.25	2.649 (8), 2.646 (8); Δ = 0.004	2.59 (1), 2.72 (1); Δ = 0.13
Guest component (G)			
Ta—Ta	2.62 (1), 2.69 (2); Δ = 0.07	2.6475 (1); Δ = 0	2.6537 (5); Δ = 0
Distance between nets	2.590 (5) and 2.717 (5)	2.6475 (1)	2.6537 (5)
Interaction between H and G			
Ta_G–Ta_H:			
Range	2.857 (6)–3.404 (7); Δ = 0.547	2.924 (3)–3.336 (3); Δ = 0.412	2.926 (18)–3.383 (13); Δ = 0.457
Average	⟨3.142⟩	⟨3.112⟩	⟨3.137⟩
Differentiation of Ta_G—Ta_H:			
$Ta5_G$—Ta_H	⟨3.122⟩	⟨3.133⟩	⟨3.122⟩
$Ta6_G$—Ta_H	⟨3.163⟩	⟨3.128⟩	⟨3.152⟩
Δ	0.041	0.005	0.03

maximum of the residual electron density and improve the R factors (Table 7). There is a difference between RT-I and RT-II: in RT-I, $M1$ and $M2$ positions show the same population while the population of $M1$ is twice the population of $M2$ in RT-II. This difference is clearly seen in Fig. 2. Note that the $M1$ and $M2$ positions are located in the net of H just between the guest atoms.

It should be mentioned that the residual electron density maps calculated for the LT and RT-II structure in the lower space group $P2_z11$ reproduce all the main features under discussion.

The nature of these additional maxima is not completely clear. However, if we believe that they are generated by structural defects, then it can be concluded that these defects are more ordered at 120 K than at room temperature, as the structure loses one defect position ($M2$) upon cooling, which is recovered after heating. The recovery of the defect state is not reversible after cooling and rewarming, $M2$ is half $M1$ at room temperature. Numerical estimation of the $M1$ + $M2$ population shows that the structure keeps the total amount of defects (atoms per a unit cell) as approximately constant: 0.08 (2), before cooling 0.06 (1), at 120 K 0.12 (4) after cooling and rewarming.

5. Discussion

5.1. Structure of β-Ta under the RT–LT–RT phase transition

The tetragonal β-Ta phase is not an equilibrium phase in the pressure–temperature (P–T) state diagram of Ta (Young, 1991). Heating this phase at ∼1000 K results in a transformation from β-Ta into α-Ta (Moseley & Seabrook, 1973). The present investigation shows that there is a phase transition between 293 and 120 K which is neither reversible [because the space group of the G substructure changes from $P42_1m$ at room temperature (RT-I) to $P4/mbm$ at 120 K (RT-II), which is conserved during heating back to room temperature (RT-II)] nor irreversible [because both the space group of the whole RT-I structure and the unit-cell parameters (within two standard deviations) are recovered in the RT-II structure after heating from 120 K to room temperature]. Clearly this duality is due to the composite character of this structure. The G substructure reveals an irreversible phase transition, while the transition in the H substructure seems to be reversible. The recovering of the structure defects described above confirms the reversibility of the phase transition for the H substructure.

However, the interaction between H and G should be different in RT-I and RT-II. This difference is a direct consequence of the different space groups of G and, therefore, the H structure cannot be completely identical. In order to analyse the interaction between H and G, the main characteristics of the three states of the structure were considered separately for the H and G components (Table 8).

Within the H substructure, the shortest Ta—Ta distances are observed in the plane of the net (primary Kagome net of the σ structure) pointing to the strongest Ta—Ta interaction. The shortest Ta_H—Ta_H distances [2.681 (7), 2.684 (1) and 2.715 (5) Å in RT-I, LT and RT-II, respectively] and the average value (2.781, 2.790 and 2.793 Å RT-I, LT and RT-II, respectively) are significantly shorter than the distance in α-Ta

Table 9
Possible combinations of the host (H; the highest space group $P4_2/mnm$) and the guest (G; the highest space group $P4/mbm$, $c_G = 0.5c_H$) components: absences (Abs); common space group (SpGr) taking into account a possible shift between the H and G origins (OS).

The generally accepted atomic notations $A_2B_4C_8D_8E_8$ (H = $A_2B_4C_8D_8$; G = E_8) after Frank & Kasper (1959) are used. The symbol ● indicates variants of a composite structure for which symmetry does not conform to experimental systematic absences.

	Space group, systematic absence and Wyckoff positions for H component (A, B, C and D atoms)						
Space group, systematic absence and Wyckoff positions for G component (E atoms)	$P4_2/mnm$ [$P4_2nm$].† $0kl$, $k + l \neq 2n$; $00l$, $l \neq 2n$; $h00$, $h \neq 2n$. *A*: $2a$(0,0,0); *B*: $4g(x,-x,0)$; both *C* and *D*: $8i(x,y,0)$	$P4_222$. $00l$, $l \neq 2n$; $h00$, $h \neq 2n$. *A*: $2a$(0,0,0); *B*: $4e(x,x,0)$; both *C* and *D*: $8g(x,y,z)$, $z \simeq 0$	$P4_2/m$[$P4_2$].† $00l$, $l \neq 2n$. *A*: $2c$(0,1/2,0); *B*: $4j(x,y,0)$, $y \simeq x + 1/2$; both *C* and *D*: $4j(x,y,0)$ $x2$	$P\bar{4}n2$. $0kl$, $k + l \neq 2n$; $00l$, $l \neq 2n$; $h00$, $h \neq 2n$. *A*: $2d$(1/2,0,1/4); *B*: $4f(x,1/2 - x,1/4)$; both *C* and *D*: $8i(x,y,z)$, $z \simeq 1/4$	$P\bar{4}2_1m$. $h00$, $h \neq 2n$. *A*: $2c$(1/2,0,z); *B*: $4e(x,x + 1/2,z)$; both *C* and *D*: $8f(x,y,z)$; $z \simeq 1/4$ everywhere	$P\bar{4}$. No reflection conditions. *A*: $2g$(1/2,0,z); *B*: $4h(x,y,z)$, $y \simeq x + 1/2$; both *C* and *D*: $4h(x,y,z)$ $x2$; $z \simeq 1/4$ everywhere
$c_G = c_H$							
$P4/mnc$ [$P4nc$].† $0kl$, $k + l \neq 2n$; $00l$, $l \neq 2n$; $h00$, $h \neq 2n$; hhl, $l \neq 2n$. *E*: $8h(x,y,0)$, $y \simeq x + 1/2$	Abs: $0kl$, $k + l \neq 2n$; $00l$, $l \neq 2n$; $h00$, $h \neq 2n$. *OS*: (0,1/2,1/4). SpGr: $P\bar{4}n2$ [$P2n1$]‡	Abs: $00l$, $l \neq 2n$; $h00$, $h \neq 2n$. OS: (0,1/2,1/4). SpGr: $P212$ [$P211$]‡	Abs: $00l$, $l \neq 2n$. OS: (0,0,1/4). SpGr: $P\bar{4}$ [$P211$]‡	Abs: $0kl$, $k + l \neq 2n$; $00l$, $l \neq 2n$; $h00$, $h \neq 2n$. OS: (0,0,0). SpGr: $P\bar{4}n2$ [$P2n1$]‡	Abs: $h00$, $h \neq 2n$. OS: (0,0,0). SpGr: $P\bar{4}$ [$P211$]‡	Abs: none. OS: (0,0,0). SpGr: $P\bar{4}$ [$P211$]‡
$P4_2/mbc$ [$P4_2bc$].† $0kl$, $k \neq 2n$; $00l$, $l \neq 2n$; $h00$, $h \neq 2n$; hhl, $l \neq 2n$. *E*: $8h(x,y,0)$, $y \simeq x + 1/2$	Abs: $00l$, $l \neq 2n$; $h00$, $h \neq 2n$; $0kl$, $l = 2n$ if $k = 2n + 1$. *OS*: (0,1/2,1/4). SpGr: $P4_22_12$ [$P4_2$]‡	Abs: $00l$, $l \neq 2n$; $h00$, $h \neq 2n$. OS: (0,1/2,1/4). SpGr: $P4_22_12$ [$P4_2$]‡	Abs: $00l$, $l \neq 2n$. OS: (0,0,1/4). SpGr: $P4_2$ [$P4_2$]‡	Abs: $00l$, $l \neq 2n$; $h00$, $h \neq 2n$; $0kl$, $l = 2n$ if $k = 2n + 1$. OS: (0,0,0). SpGr: $P212$ [$P211$]‡	Abs: $h00$, $h \neq 2n$. *OS*: (0,0,0). SpGr: $P221$ [$P211$]‡	Abs: none. OS: (0,0,0). SpGr: $P211$ [$P211$]‡
$P4/mbm$ [$P4bm$].† $0kl$, $k \neq 2n$; $h00$, $h \neq 2n$. I. *E*: $8k(x,x + 1/2,z)$, $z \simeq 1/4$. II. *E*1: $4g(x_1,x_1 + 1/2,0)$; *E*2: $4h(x_2,x_2 + 1/2,1/2)$, $x_2 \simeq x_1$	Abs: $h00$, $h \neq 2n$; $0kl$, $l = 2n$ if $k = 2n + 1$. ●I. OS: (0,1/2,0). SpGr: $P212$ [$P211$]‡ II. OS: (0,1/2,1/4). SpGr: $P2/m12/m$ [$P21m$].‡ II. OS: (0,1/2,1/4). SpGr: $P\bar{4}2_1m$ [$P21m$]‡	Abs: $h00$, $h \neq 2n$. ●I. OS: (0,1/2,0). SpGr: $P212$ [$P211$]‡ II. OS: (0,1/2,1/4). SpGr: $P22_11$ [$P211$]‡	Abs: none. I. OS: (0,0,0). SpGr: $P2/m11$ [$P211$]‡ II. OS: (0,0,1/4). SpGr: $P\bar{4}$ [$P211$]‡	Abs: $h00$, $h \neq 2n$; $0kl$, $l = 2n$ if $k = 2n + 1$. ●I. OS: (0,0,1/4). SpGr: $P212$ [$P211$]‡ ●II. OS: (0,0,0). SpGr: $P\bar{4}$ [$P211$]‡	Abs: $h00$, $h \neq 2n$. ●I. OS: (0,0,1/4). SpGr: $P21m$ [$P21m$]‡ II. OS: (0,0,0). SpGr: $P\bar{4}2_1m$[$P21m$]‡	Abs: none. I. OS: (0,0,1/4). SpGr: $P211$ [$P211$]‡ II. OS: (0,0,0). SpGr: $P\bar{4}$ [$P211$]‡
$P4_2/mnm$ [$P4_2nm$].† $0kl$, $k + l \neq 2n$; $00l$, $l \neq 2n$; $h00$, $h \neq 2n$. I. *E*: $8j(x,x,z)$, $z \simeq 1/4$. II. *E*1: $4g(x_1,-x_1,0)$; *E*2: $4f(x_2,x_2,0)$, $x_2 \simeq x_1 + 1/2$	Abs: $0kl$, $k + l \neq 2n$; $00l$, $l \neq 2n$; $h00$, $h \neq 2n$. I. OS: (0,0,0). SpGr: $P4_2/mnm$ [$P4_2nm$]‡ II. OS: (0,0,1/4). SpGr: $P4_2nm$ [$P4_2nm$]‡	Abs: $00l$, $l \neq 2n$; $h00$, $h \neq 2n$. I. OS: (0,0,0). SpGr: $P4_22_12$ [$P4_2$]‡. ●II. OS: (0,0,1/4). SpGr: $P4_2$ [$P4_2$]‡	Abs: $00l$, $l \neq 2n$. I. OS: (0,1/2,0). SpGr: $P4_2/m$ [$P4_2$].‡ II. OS: (0,1/2,1/4). SpGr: $P4_2$ [$P4_2$]‡	Abs: $0kl$, $k + l \neq 2n$; $00l$, $l \neq 2n$; $h00$, $h \neq 2n$. I. OS: (0,1/2,1/4). SpGr: $P\bar{4}n2$ [$P2n1$].‡ II. OS: (0,1/2,0). SpGr: $P2n1$[$P2n1$]‡	Abs: $h00$, $h \neq 2n$. I. OS: (0,1/2,1/4). SpGr: $P\bar{4}2_1m$[$P21m$].‡● $P21m$[$P21m$]‡	Abs: none. I. OS: (0,1/2,1/4). SpGr: $P\bar{4}$ [$P211$]‡ II. OS: (0,1/2,0). SpGr: $P211$ [$P211$]‡
$P\bar{4}n2$. $0kl$, $k + l \neq 2n$; $00l$, $l \neq 2n$; $h00$, $h \neq 2n$. I. *E*: $8i(x,y,z)$, $z \simeq 0$, $y \simeq x + 1/2$. II. *E*1: $4f(x_1,1/2 - x_1,1/4)$; *E*2: $4g(x_2,1/2 + x_2,1/4)$, $x_1 \simeq x_2 + 1/2$	Abs: $0kl$, $k + l \neq 2n$; $00l$, $l \neq 2n$; $h00$, $h \neq 2n$. I. OS: (0,1/2,1/4). SpGr: $P\bar{4}n2$ [$P2n1$].‡ II. OS: (0,1/2,0). SpGr: $P2n1$ [$P2n1$]‡	Abs: $00l$, $l \neq 2n$; $h00$, $h \neq 2n$. ●I. OS: (0,1/2,1/4). SpGr: $P212$ [$P212$]‡ II. OS: (0,1/2,0). SpGr: $P211$ [$P211$]‡	Abs: $00l$, $l \neq 2n$. ●I. OS: (0,0,1/4). SpGr: $P\bar{4}$ [$P211$]‡ II. OS: (0,0,0). SpGr: $P211$ [$P211$]‡	Abs: $0kl$, $k + l \neq 2n$; $00l$, $l \neq 2n$; $h00$, $h \neq 2n$. I. OS: (0,0,0). SpGr: $P\bar{4}n2$ [$P2n1$]‡ II. OS: (0,0,1/4). SpGr: $P2n1$ [$P2n1$]‡	Abs: $h00$, $h \neq 2n$. ●I. OS: (0,0,0). SpGr: $P\bar{4}$ [$P211$]‡ II. OS: (0,0,1/4). SpGr: $P211$ [$P211$]‡	Abs: none. I. OS: (0,0,0). SpGr: $P\bar{4}$ [$P211$]‡ II. OS: (0,0,1/4). SpGr: $P211$ [$P211$]‡
$P\bar{4}b2$. $0kl$, $k \neq 2n$; $h00$, $h \neq 2n$. *E*: $8i(x,y,z)$, $z \simeq 1/4$, $y \simeq x + 1/2$	●Abs: $h00$, $h \neq 2n$ $0kl$, $l = 2n$ if $k = 2n + 1$. OS: (0,1/2,0). SpGr: $P212$ [$P211$]‡	●Abs: $h00$, $h \neq 2n$. OS: (0,1/2,0). SpGr: $P212$ [$P211$]‡	Abs: none. OS: (0,0,0). SpGr: $P211$ [$P211$]‡	Abs: $h00$, $h \neq 2n$ $0kl$, $l = 2n$ if $k = 2n + 1$. OS: (0,0,1/4). SpGr: $P22_11$ [$P211$]‡	●Abs: $h00$, $h \neq 2n$. OS: (0,0,1/4). SpGr: $P211$ [$P211$]‡	Abs: none. OS: (0,0,1/4). SpGr: $P211$ [$P211$]‡
$P\bar{4}2_1m$. $h00$, $h \neq 2n$. *E*1: $4e(x_1,1/2 + x_1,z_1)$; *E*2: $4e(x_2,1/2 + x_2,z_2)$, $x_1 \simeq x_2$. I. $z_1 \simeq 0$, $z_2 \simeq 1/2$. II. $z_1 \simeq 1/4$, $z_2 \simeq 3/4$	Abs: $h00$, $h \neq 2n$. I. OS: (0,1/2,1/4). SpGr: $P\bar{4}2_1m$ [$P21m$]‡. ●II. OS: (0,1/2,0). SpGr: $P21m$ [$P21m$]‡	Abs: $h00$, $h \neq 2n$; I. OS: (0,1/2,1/4). SpGr: $P22_11$[$P211$]‡ ●II. OS: (0,1/2,0). SpGr: $P211$ [$P211$]‡	Abs: none. I. OS: (0,0,1/4). SpGr: $P\bar{4}$ [$P211$]‡ II. OS: (0,0,0). SpGr: $P211$ [$P211$]‡	Abs: $h00$, $h \neq 2n$. ●I. OS: (0,0,0). SpGr: $P\bar{4}$ [$P211$]‡ ●II. OS: (0,0,1/4). SpGr: $P211$[$P211$]‡	Abs: $h00$, $h \neq 2n$. I. OS: (0,0,0). SpGr: $P\bar{4}2_1m$ [$P21m$]‡ ●II. OS: (0,0,1/4). SpGr: $P21m$ [$P21m$]‡	Abs: none. I. OS: (0,0,0). SpGr: $P\bar{4}$ [$P211$]‡ II. OS: (0,0,1/4). SpGr: $P211$ [$P211$]‡
$P\bar{4}2_1c$. $00l$, $l \neq 2n$; $h00$, $h \neq 2n$; hhl, $l \neq 2n$. *E*: $8e(x,y,z)$, $y \simeq x + 1/2$. I. $z \simeq 0$. II. $z \simeq 1/4$	Abs: $00l$, $l \neq 2n$; $h00$, $h \neq 2n$. ●I. OS: (0,1/2,1/4). SpGr: $P\bar{4}$ [$P211$].‡ ●II. OS: (0,1/2,0). SpGr: $P22_11$ [$P211$]‡	Abs: $00l$, $l \neq 2n$; $h00$, $h \neq 2n$. ●I. OS: (0,1/2,1/4). SpGr: $P211$ [$P211$].‡ ●II. OS: (0,1/2,0). SpGr: $P22_11$ [$P211$]‡	Abs: $00l$, $l \neq 2n$. ●I. OS: (0,0,1/4). SpGr: $P\bar{4}$[$P211$].‡ ●II. OS: (0,0,0). SpGr: $P211$ [$P211$]‡	Abs: $00l$, $l \neq 2n$; $h00$, $h \neq 2n$. ●I. OS: (0,0,0). SpGr: $P\bar{4}$ [$P211$].‡ ●II. OS: (0,0,1/4). SpGr: $P211$ [$P211$]‡	Abs: $h00$, $h \neq 2n$. ●I. OS: (0,0,0). SpGr: $P\bar{4}$ [$P211$].‡ II. OS: (0,0,1/4). SpGr: $P22_11$ [$P211$]‡	Abs: none. I. OS: (0,0,0). SpGr: $P\bar{4}$ [$P211$].‡ II. OS: (0,0,1/4). SpGr: $P211$[$P211$]‡
$P4_22_12$. $00l$, $l \neq 2n$; $h00$, $h \neq 2n$. *E*: $8g(x,y,z)$, $x \simeq y$, $z \simeq 1/4$	Abs: $00l$, $l \neq 2n$; $h00$, $h \neq 2n$. OS: (0,0,0). SpGr: $P4_22_12$ [$P4_2$]†	Abs: $00l$, $l \neq 2n$; $h00$, $h \neq 2n$. OS: (0,0,0). SpGr: $P4_22_12$ [$P4_2$]‡	Abs: $00l$, $l \neq 2n$. OS: (0,1/2,0). SpGr: $P4_2$ [$P4_2$]‡	● Abs: $00l$, $l \neq 2n$; $h00$, $h \neq 2n$. OS: (0,1/2,1/4). SpGr: $P212$ [$P211$]‡	Abs: $h00$, $h \neq 2n$. OS: (0,0,1/4). SpGr: $P22_11$[$P211$]‡	Abs: none. OS: (0,1/2,1/4). SpGr: $P211$[$P211$]‡

Table 9 (continued)

	Space group, systematic absence and Wyckoff positions for H component (*A*, *B*, *C* and *D* atoms)					
$P4/m$ [$P4$].† No reflection conditions. I. *E*: $8l(x,y,z)$, $z \simeq 1/4$, $y \simeq x + 1/2$. II. *E*1: $4k(x_1,y_1,1/2)$, $y_1 \simeq x_1 + 1/2$; *E*2: $4j(x_2,y_2,0)$,$y_2 \simeq x_2 + 1/2$; $x_1 \simeq x_2$	Abs: none. I. OS: (0, 1/2,0). SpGr: $P2/m11$[$P211$].‡ II. OS: (0,1/2,1/4). SpGr: $P\bar{4}$ [$P211$]‡	Abs: none. I. OS: (0, 1/2,0). SpGr: $P211$ [$P211$].‡ II. OS: (0, 1/2,1/4). SpGr: $P211$ [$P211$]‡	Abs: none. I. OS: (0,0,0). SpGr: $P2/m11$ [$P211$].‡ II. OS: (0,0,1/4). SpGr: $P\bar{4}$ [$P211$]‡	Abs: none. I. OS: (0,0,1/4). SpGr: $P211$ [$P211$]‡ II. OS: (0,0,0). SpGr: $P\bar{4}$ [$P211$]‡	Abs: none. I. OS: (0,0,1/4). SpGr: $P211$ [$P211$]‡ II. OS: (0,0,0). SpGr: $P\bar{4}$ [$P211$]‡	Abs: none. I. OS: (0,0,1/4). SpGr: $P211$ [$P211$]‡ II. OS: (0,0,0). SpGr: $P\bar{4}$ [$P211$]‡
$P4_2/m$ [$P4_2$].† $00l$, $l \neq 2n$. I. *E*: $8l(x,y,z)$, $z \simeq 1/4$, $y \simeq x + 1/2$. II. *E*1: $4j(x_1,y_1,0)$, $y_1 \simeq x_1 + 1/2$; *E*2: $4k(x_2,y_2,1/2)$, $y_2 \simeq x_2 + 1/2$; $x_2 \simeq x_1$	Abs: $00l$, $l \neq 2n$. I. OS: (0,1/2,0). SpGr: $P4_2/m$ [$P4_2$].‡ II. OS: (0, 1/2,1/4). SpGr: $P4_2$ [$P4_2$]‡	Abs: $00l$, $l \neq 2n$. I. OS: (0,1/2,0). SpGr: $P4_2$ [$P4_2$].‡ II. OS: (0,1/2,1/4). SpGr: $P4_2$ [$P4_2$]‡	Abs: $00l$, $l \neq 2n$. I. OS: (0,0,0). SpGr: $P4_2/m$ [$P4_2$].‡ II. OS: (0,0,1/4). SpGr: $P4_2$ [$P4_2$]‡	Abs: $00l$, $l \neq 2n$. ● I. OS: (0,0,1/4). SpGr: $P\bar{4}$ [$P211$].‡● II. OS: (0,0,0). SpGr: $P211$ [$P211$]‡	*Abs*: none. I. OS: (0,0,1/4). SpGr: $P\bar{4}$ [$P211$].‡ II. OS: (0,0,0). SpGr: $P211$ [$P211$]‡	Abs: none. I. OS: (0,0,1/4). SpGr: $P\bar{4}$ [$P211$]‡ II. OS: (0,0,0). SpGr: $P211$ [$P211$]‡
$P\bar{4}$. No reflection conditions. *E*1: $4h(x_1,y_1,z_1)$, $y_1 \simeq x_1 + 1/2$; *E*2: $4h(x_2,y_2,z_2)$, $y_2 \simeq x_2 + 1/2$; $x_1 \simeq x_2$; $z_2 \simeq z_1 + 1/2$. I. $z_1 \simeq 0$. II. $z_1 \simeq 1/4$ $c_G = 1/2c_H$	Abs: none. I. OS: (0, 1/2,1/4). SpGr: $P\bar{4}$ [$P211$].‡ II. OS: (0, 1/2,0). SpGr: $P211$ [$P211$]‡	Abs: none. I. OS: (0, 1/2,1/4). SpGr: $P211$ [$P211$].‡ II. OS: (0,1/2,0). SpGr: $P211$ [$P211$]‡	Abs: none. I. OS: (0,0,1/4). SpGr: $P\bar{4}$ [$P211$].‡ II. OS: (0,0,0) SpGr: $P211$ [$P211$]‡	Abs: none. I. OS: (0,0,0). SpGr: $P\bar{4}$ [$P211$].‡ II. OS: (0,0,1/4). SpGr: $P211$ [$P211$]‡	Abs: none. I. OS: (0,0,0). SpGr: $P\bar{4}$ [$P211$].‡ II. OS: (0,0,1/4). SpGr: $P211$ [$P211$]‡	Abs: none. I. OS: (0,0,0). SpGr: $P\bar{4}$ [$P211$].‡ II. OS: (0,0,1/4). SpGr: $P211$ [$P211$]‡
$P4/mbm$ [$P4bm$].† hkl, $l \neq 2n$; $0kl$, $k \neq 2n$; $0kl$, $k + l \neq 2n$; $00l$, $l \neq 2n$; $h00$, $h \neq 2n$. *E*: $4g(x,x + 1/2,0)$	Abs: $0kl$, $k + l \neq 2n$; $00l$, $l \neq 2n$; $h00$, $h \neq 2n$. OS: (0,1/2, $1/4_H$). SpGr: $P4_2/mnm$ [$P4_2nm$]‡	Abs: $00l$, $l \neq 2n$; $h00$, $h \neq 2n$. OS: (0,1/2, $1/4_H$). SpGr: $P4_22_12$ [$P4_2$]‡	Abs: $00l$, $l \neq 2n$. OS: (0,0,$1/4_H$). SpGr: $P4_2/m$ [$P4_2$]‡	Abs: $0kl$, $k + l \neq 2n$; $00l$, $l \neq 2n$; $h00$, $h \neq 2n$. OS: (0,0,0). SpGr: $P\bar{4}n2$ [$P2n1$]‡	Abs: $h00$, $h \neq 2n$. OS: (0,0,0). SpGr: $P\bar{4}2_1m$ [$P21m$]‡	Abs: none. OS: (0,0,0). SpGr: $P\bar{4}$ [$P211$]‡
$P\bar{4}2_1m$. hkl, $l \neq 2$; $h00$, $h \neq 2n$; $00l$, $l \neq 2n$; hhl, $l \neq 2n$; $0kl$, $l \neq 2n$. *E*: $4e(x,1/2 + x,z)$, $z \simeq 0$	Abs: $h00$, $h \neq 2n$; $00l$, $l \neq 2n$; $0kl$, $k \neq 2n + 1$ if $l \neq 2n + 1$. OS: (0,1/2,$1/4_H$). SpGr: $P\bar{4}2_1m$ [$P21m$]‡	● Abs: $h00$, $h \neq 2n$; $00l$, $l \neq 2n$. OS: (0, 1/2,$1/4_H$). SpGr: $P22_11$ [$P211$]‡	● Abs: $00l$, $l \neq 2n$. OS: (0,0,$1/4_H$). SpGr: $P\bar{4}$ [$P211$]‡	● Abs: $h00$, $h \neq 2n$; $00l$, $l \neq 2n$; $0kl$, $k \neq 2n+1$ if $l \neq 2n + 1$. OS: (0,0,$1/4_H$). SpGr: $P\bar{4}$ [$P211$]‡	Abs: $h00$, $h \neq 2n$. OS: (0,0,0). SpGr: $P\bar{4}2_1m$ [$P21m$]‡	Abs: none. OS: (0,0,0). SpGr: $P\bar{4}$ [$P211$]‡
$P4/m$ [$P4$].† hkl, $l \neq 2n$; $00l$, $l \neq 2n$; hhl, $l \neq 2n$. *E*: $4k(x,y,1/2)$, $y \simeq x + 1/2$	Abs: $00l$, $l \neq 2n$. OS: (0,1/2,0). SpGr: $P4_2/m$ [$P4_2$]‡	Abs: $00l$, $l \neq 2n$. OS: (0,1/2,0). SpGr: $P4_2$ [$P4_2$]‡	Abs: $00l$, $l \neq 2n$. OS: (0,0,0). SpGr: $P4_2/m$ [$P4_2$]‡	● Abs: $00l$, $l \neq 2n$. OS: (0,0,$1/4_H$). SpGr: $P\bar{4}$ [$P211$]‡	Abs: none. OS: (0,0, $1/4_H$). SpGr: $P\bar{4}$ [$P211$]‡	Abs: none. OS: (0,0, $1/4_H$). SpGr: $P\bar{4}$ [$P211$]‡
$P\bar{4}b2$. hkl, $l \neq 2n$; $0kl$, $k \neq 2n$; $0kl$, $k + l \neq 2n$; $h00$, $h \neq 2n$; $00l$, $l \neq 2n$. *E*: $4g(x,1/2 + x,0)$	Abs $0kl$, $k + l \neq 2n$; $h00$, $h \neq 2n$; $00l$, $l \neq 2n$. OS: (0,1/2, $1/4_H$). SpGr: $P\bar{4}n2$ [$P2n1$]‡	● Abs: $h00$, $h \neq 2n$; $00l$, $l \neq 2n$. OS: (0, 1/2,1/4_H). SpGr: $P212$[$P211$]‡	● Abs: $00l$, $l \neq 2n$. OS: (0,0,$1/4_H$). SpGr: $P\bar{4}$ [$P211$]‡	Abs:$0kl$, $k + l \neq 2n$; $h00$, $h \neq 2n$; $00l$, $l \neq 2n$. OS: (0,0,0). SpGr: $P\bar{4}n2$ [$P2n1$]‡	● Abs: $h00$, $h \neq 2n$. OS: (0,0,0). SpGr: $P\bar{4}$ [$P211$]‡	Abs: none. OS: (0,0,0). SpGr: $P\bar{4}$ [$P211$]‡
$P\bar{4}$. hkl, $l \neq 2n$; $00l$, $l \neq 2n$. *E*: $4h(x,y,z)$, $y \simeq x + 1/2$, $z \simeq 0$	● Abs: $00l$, $l \neq 2n$. OS: (0,1/2,1/4_H). SpGr: $P\bar{4}$ [$P211$]‡	● Abs: $00l$, $l \neq 2n$; OS: (0,1/2,1/4_H). SpGr: $P211$, 1 [$P211$]‡	● Abs: $00l$, $l \neq 2n$. OS: (0,0,$1/4_H$). SpGr: $P\bar{4}$ [$P211$]‡	● Abs: $00l$, $l \neq 2n$; OS: (0,0,0). SpGr: $P\bar{4}$ [$P211$]‡	Abs: none. OS: (0,0,0). SpGr: $P\bar{4}$ [$P211$]‡	Abs: none. OS: (0,0,0). SpGr: $P\bar{4}$[$P211$]‡

† Wyckoff positions are listed for the centrosymmetric space group only. ‡ Space group compatible with a composite structure which contains a non-centrosymmetric component and/or difference between the origins of H and G.

(2.86 Å); the last value being closely related to the longest distance in the net [2.893 (7), 2.882 (1) and 2.891 (5) Å in RT-I, LT and RT-II, respectively]. In RT-II, the Ta atoms are more evenly distributed than in RT-I [the scatterings of the distances are $\Delta = 0.176$ Å in RT-II and $\Delta = 0.212$ Å in RT-I; the maximal deflections from the average plane of a net are 0.048 (7) Å in RT-II and 0.09 (2) Å in RT-I] owing to the increase of the shorter distances (the average values are ⟨2.793 Å⟩ in RT-II and ⟨2.781 Å⟩ in RT-I). The even distribution of the atoms and the increase of the average distances in the primary net of RT-II compared with RT-I seem to be correlated with the change of space group of G from $P\bar{4}2_1m$ in RT-I to $P4/mbm$ ($c_G = 0.5c_H$) in RT-II, because both of these characteristics are present in the LT structure which has space group $P4/mbm$ ($c_G = 0.5c_H$), similar to RT-II. The average distance in LT, ⟨2.790 Å⟩, is practically equal to that in RT-II, ⟨2.793 Å⟩ despite a temperature reduction of the longer distances in LT.

The longest Ta—Ta distances (2.84–3.35 Å) are observed between the primary nets. These distances correspond to those in α-Ta (2.86 and 3.30 Å). The average value is shorter in RT-II (⟨3.114 Å⟩) than in RT-I (⟨3.131 Å⟩), despite the increase of the longer distances in RT-II [up to 3.349 (2) Å] in comparison

with RT-I [the longest is 3.301 (7) Å]. The shorter average distance between atoms of the primary nets in RT-II can be interpreted as a slight increase of the Ta_H—Ta_H interactions between the nets in RT-II, which is maintained when heating from 120 K (⟨3.119 Å⟩ in LT) to room temperature in the knowledge that the space group $P4/mbm$ of G does not change.

The equalization of the distances in the primary net (the group of the shortest distances, 2.68–2.89 Å, of H described above) and the decrease of the distances between these nets (group of the longest distances, 2.84–3.35 Å) are linked to the relatively stronger Ta_H–Ta_H interaction within the H substructure of RT-II in comparison to RT-I.

In the plane of the secondary net of substructure G, there is no Ta_G–Ta_G interaction and the minimal distance is equal to 5.29 Å. The short distance between atoms is equal to the distance between the average planes of the nets, which is equal to c_G in RT-II, while all are different in RT-I. One of the distances between the average nets is too short [2.590 (5) Å] and the corresponding Ta_G–Ta_G distance is slightly longer [2.62 (1) Å]. Another distance is longer [2.717 (5) Å], with the corresponding Ta_G–Ta_G distances equal to 2.69 (2) Å. The equalization of these interatomic distances in RT-II is associated with the stabilization of the G substructure.

The differentiation of both the interatomic distances in G and the distances between the primary nets of H [2.53 (2) and 2.78 (2) Å], the deviation of atoms from the average plane of both the secondary nets of G [0.048 (5) Å] and the primary nets of H [0.09 (2) Å] are linked to the stronger interaction between G and H in RT-I than in RT-II. The shorter Ta_H–Ta_G distances only observed in the RT-I structure (∼2.86 Å checking against ∼2.93 Å in both LT and RT-II) confirm this point.

Thus, the higher symmetry space group of the G substructure is realised owing to the partial decrease of interactions between the H and G substructures.

These two substructures become even more independent at 120 K (the LT structure): both the primary nets of H and the secondary nets of G are evenly distributed along the fourfold axis and practically no differentiation of the distances along this axis can be observed (the $Ta5_G$–Ta_H distances are equal to $Ta6_G$–Ta_H). The shortening of the average value of the Ta_G–Ta_H distances in LT (⟨3.112 Å⟩ compared with ⟨3.142 Å⟩ in RT-I and ⟨3.137 Å⟩ in RT-II) is clearly associated with the lower temperature.

The temperature dependence of the structural characteristics is clearly revealed by comparing the LT and RT-II structures, both of which exhibit the same space group as G. The unit-cell parameters are reduced by 0.2%. The most temperature-sensitive Ta—Ta distances are longer than 3.30 Å: the temperature reduction of the maximal distance observed between the primary Kagome nets of H is ∼1.7%; between the primary and secondary nets (between the atoms of H and G): ∼1.4%. In comparison, the temperature reduction of the shortest distance in the structure (Ta_G–Ta_G in the G substructure) is only 0.17%. All these values refer mainly to the c direction. Therefore, it can be concluded that the thermal effect is higher for the H than for the G substructure along this direction. Below 120 K an incommensurately composite structure along this direction might be possible for β-Ta.

6. Conclusions

The single-crystal investigation of the self-hosting σ-structure of β-Ta at 293 and 120 K shows that a σ-structure is a particular two-component composite where the components have the same (or a multiple) lattice constants but different space groups: the space group of both the host (H) and guest component (G) causes systematic absences. Their intersection corresponds to the observed diffraction data.

The symmetry of a σ-structure can be described with three space groups that characterize the two components and the composite structure. The highest symmetry of a σ-structure can be described as [H: $P4_2/mnm$; G: $P4/mbm$ ($c_G = 0.5c_H$); composite structure: $P4_2/mnm$].

In the β-Ta structure, the symmetry of the two components can be identified by the thermal process 293 K (RT-I) ⇒ 120 K (LT) ⇒ 293 K (RT-II): [H: $P\bar{4}2_1m$; G: $P\bar{4}2_1m$; composite structure: $P\bar{4}2_1m$] ⇒ [H: $P\bar{4}$; G: $P4/mbm$ ($c_G = 0.5c_H$); composite structure: $P\bar{4}$] ⇒ [H: $P\bar{4}2_1m$; G: $P4/mbm$ ($c_G = 0.5c_H$); composite structure: $P\bar{4}2_1m$].

The phase transition is reversible with respect to the H substructure and irreversible with respect to the G substructure.

The low-temperature phase transition is linked to a partial suppression of the interaction between the H and G components.

APPENDIX *A*
The composite symmetry of a tetragonal σ-structure

A1. Motivation

The determination of the symmetry of a σ-structure is not a trivial task, as evidenced by the present investigation of the β-Ta structure and previous work on β-U (Lawson *et al.*, 1988). The problem derives from the fact that the σ-structure is a two-component composite (see main text) where the components have the same (or a multiple) lattice constants but different space groups: the space group of both the host component (H) and guest component (G) cause systematic absences, and the observed absences in the diffraction data are because of their intersection. These absences cannot help choose the space group of the combination H + G. The space group of a single component generates at least all of them and may produce more, while the space group of H + G generates at most the absences of a single component and may produce less (even none). The diffraction pattern may also show non-space group absences.

The symmetry of the two-component composite is characterized by three space groups: space groups of both components and of their combination. The information obtained from experiment is not sufficient to identify any one of them. Therefore, the determination of the correct symmetry

requires a detailed theoretical analysis. Without such an analysis, no σ-structure can be correctly refined, not even β-U and β-Ta.

A2. Method and results

A2.1. Selection of the component space groups and their combinations. The following criteria were selected for the analysis of all possible H + G combinations leading to a composite structure:

(i) The space groups of both H and G should be tetragonal. A lower symmetry is in principle not impossible, but we limit our considerations to the tetragonal system which is accepted for a σ-structure type.

(ii) The space group of H should be $P42/mnm$ (highest available symmetry) or one of its non-isomorphic subgroups.

(iii) The space group of G should be $P4/mbm$ with the lattice parameter $c_G = 0.5c_H$ (highest available symmetry), or one of its non-isomorphic subgroups, or an isomorphic subgroup of lower index ($c_G = c_H$).

(iv) The fourfold axis of H coincides with the fourfold axis of G. However, it is not necessary for the origins to be common. Shifts of $0.5c_H$ or $0.25c_H$ between the origins are possible.

A2.2. Characteristics of H and G components. In order to describe the σ-structure type we use the generally accepted alphabetic notation (after Frank & Kasper, 1959) for the atomic positions: the 30 atoms located in the unit cell are symbolized by $A_2B_4C_8D_8E_8$, where $A_2B_4C_8D_8$ refer to H and E_8 refers to G; every letter corresponds to one atomic position in space group $P4_2/mnm$.

The results of our analysis are listed in Table 9. The possible space groups of H are listed in the upper line together with their systematic absences and details of the atomic positions of the σ-structure. The analogous characteristics of G are listed in the left column. The h, k, l indices refer always to the common unit cell ($c = c_H$). If the systematic absences of a centrosymmetric group ($P4_2/mnm$, for example) are equal to the absences of the non-centrosymmetric group, which differ only by a centre of inversion ($P4_2nm$, in the example), these groups are listed together in the table; the atomic positions however refer to the centrosymmetric group.

The coordinates of every atomic position are determined either approximately or by the site symmetry. Some space groups of G allow two variants (numbered as I and II in the table) for E atomic position(s).

A2.3. Characteristics of the composite structures. Every cell of the table contains information about a composite structure which is a combination of H and G given in the upper line and left column, respectively. This information consists of:

(i) Systematic absences (Abs): They are obtained as the intersection ('H.AND.G') of the absences of H and G. Besides the usual space-group absences, some composite structures generate special absences resulting from different rules for the same group of reflections: absences $0kl$, $k \neq 2n$ in G and $0kl$, $k + l \neq 2n$ in H together produce absences $0kl$, $l = 2n$ and $k \neq 2n + 1$ in the composite structure. These special absences can be of great use in limiting the choice of variants that agree with the diffraction experiment. The subset of reflections extracted from the experimental data as absences 'H − (H.AND.G)' [or 'G − (H.AND.G)'] can be used for an independent refinement of G [or H].

(ii) Shift between the origins of H and G (OS): Characteristics of the atomic positions listed for H and G refer to the standard setting of their space groups. In the (H + G) combination, the shift between the H and G is required to keep the structure type. The OS vector is uniquely related to the atomic positions chosen for the H and G space groups. Thus, for any combination of the H and G space groups, two different combinations H + G (indicated as I and II in the table) are described if two sets of E atomic position(s) are chosen for the space group of G. The OS vector is needed to determine the space group of the H + G composite structure. The z component of any OS vector refers always to the lattice parameter $c = c_H$.

(iii) Space group of the composite structure (SpGr): This characteristic is determined by the intersection of symmetry operations of H and G taking into account the shift between their origins. As mentioned before, the space group of a composite structure cannot always be determined uniquely on the basis of observed systematic absences (these cases are indicated in the table). Moreover, the space group of a composite structure cannot be used for the structure refinement without additional restrictions resulting from the symmetries of the atomic positions in H and G. Exceptions to this rule are H + G composite structures for which the space group of H is equal to the space group of G and the lattice parameter is $c_H = c_G$. Such structures can be regarded as non-composite (normal), their space groups are given by the set of space groups available for H. It is possible that the space group of a composite structure belongs to the orthorhombic system while both H and G have tetragonal symmetry. However, the space group of a composite structure can be used for the structure refinement in order to reveal the symmetry relations among the atomic coordinates. The space group symbols are always listed in the tetragonal system even for orthorhombic groups [for example, $P22_11$ (tetragonal, $P2_z2_{1\ (x\,=\,y)}1_{(xy)}$) rather than $P22_12_1$ (orthorhombic)].

Note: A small discrepancy δ along c might be possible in an OS vector: (0, 0, δ), (0, 1/2, δ), (0, 0, 1/4 + δ), (0, 1/2, 1/4 + δ) rather than (0, 0, 0), (0, 1/2, 0), (0, 0, 1/4), (0, 1/2, 1/4). Here, and in at least one non-centrosymmetric space group in a H + G combination, the symmetry elements which are normal to the fourfold axis (mirror plane, and/or 2_1- and/or twofold axes) cannot be present in the composite structure. The corresponding space group is shown in brackets and indicated in the table.

A difference in the c_H and c_G (or $2c_G$) lattice parameters leads to a modulated composite structure which can be described by one of the H + G combinations listed in the table. A structure modulation can be detected from experimental diffraction data by the presence of satellite reflections.

A3. General scheme of a structural study

Systematic and additional absences obtained from the experimental diffraction data are compared with the Abs characteristics of the H + G combinations in order to select a set of possible variants of a composite structure.

The space group with the lowest order found in the set is used to detect specific relations among the atomic coordinates in order to estimate the possible special atomic positions in the H and G substructures.

From this information, the possible variants of the H and G space groups can be selected. The selected H + G combinations should be tested (variant by variant) by structure refinement. It should be performed with the space group of the corresponding composite structure and additional restrictions derived from the special atomic positions in the H and G space group. For some H + G combinations, it may be possible to test a choice of space group of one component using reflections that are systematically absent for the other component.

The method proposed here to investigate a σ-structure is not straightforward or easy, and the results may be ambiguous. However, the results obtained without a systematic analysis of this structure type may be incorrect and the efforts to obtain experimental diffraction data and their treatment may be in vain. For example, Lawson *et al.* (1988) concluded that β-U metal is stable between 935 and 1045 K in space group $P4_2/mnm$ on the basis of profile refinements of time-of-flight neutron diffraction data. In their article, the z coordinate of the E atomic position is equal to 0.7444 (14) at 955 K and 0.7482 (30) at 1030 K. In the first case, the deviation of this coordinate from 0.75 [from the mirror m plane normal to the fourfold axis in space group $P4/mbm$ ($c_G = 0.5c_H$) of the G component] is significantly larger than the standard deviation. This confirms the space group selected for the whole structure and thus also for each component. In the second case, the E position is located on the mirror plane within one standard deviation, which confirms the composite structure described with the symmetry: G: $P4/mbm$ ($c_G = 0.5c_H$); H: $P4_2/mnm$; composite structure: $P4_2/mnm$. Therefore, β-U metal is not completely stable between 1045 and 935 K. The claim that 'This finding ends a long controversy dating back to the 1950's' (Lawson *et al.*, 1988) concerning β-U metal, is perhaps slightly overstated.

A4. An example: study of the symmetry of LT β-Ta

The diffraction data obtained in the present investigation of β-Ta at 120 K (the LT structure) do not show any systematic absences. According to the systematic analysis described above, 54 H + G combinations agree with this condition. The lowest symmetry detected among the possible composite structure space groups is $P112$. The structure refinement was performed in this space group. The relations between the coordinates of all the atoms agreed closely with the $\bar{4}$ axis. This justifies the refinement of the structure in space group $P\bar{4}$ which belongs to the set of possible H + G combinations. This refinement clearly showed that two positions of E atoms in G actually merge into the site $4g(x,x + 0.5,0)$ of space group $P4/mbm$ ($c_G = 0.5c_H$). There is only one H + G combination which (a) does not generate any systematic absence and (b) has space group $P4/mbm$ for the G component: H: $P\bar{4}$, G: $P4/mbm$ ($c_G = 0.5c_H$), composite structure: $P\bar{4}$.

This example shows that a unique solution can be found among the many variants, which agree with the absences in experimental diffraction data.

We thank Professor Dieter Schwarzenbach for discussions. This work is supported by the Herbette Foundation of the University of Lausanne, by the Swiss National Science Foundation (grant 20-56870.99) and by the Russian Foundation for Basic Research (grant 02-03-32982). The SNBL is also gratefully acknowledged for the low-temperature data collection.

References

Arakcheeva, A., Chapuis, G. & Grinevitch V. (2002). *Acta Cryst.* B**58**, 1–7.
Becker, P. & Coppens, P. (1974). *Acta Cryst.* A**30**, 129–147.
Bergman, G. & Shoemaker, D. P. (1954). *Acta Cryst.* **7**, 857–865.
Birkedal, H. (2000). PhD thesis. University of Lausanne, Switzerland.
Donohue, J. (1974). *The Structure of the Elements*, pp. 134–148. New York: John Wiley.
Donohue, J. & Einspahr, H. (1971). *Acta Cryst.* B**27**, 1740–1743.
Frank, F. C. & Kasper, J. S. (1958). *Acta Cryst.* **11**, 184–189.
Frank, F. C. & Kasper, J. S. (1959). *Acta Cryst.* **12**, 483–488.
Lawson, A. C., Olsen, C. E., Richardson Jr, J. W., Mueller, M. H. & Lander, G. H. (1988). *Acta Cryst.* B**44**, 89–96.
McMahon, M. I., Degtyareva, O. & Nelmes, R. J. (2000). *Phys. Rev. Lett.* **85**, 4896–4899.
McMahon, M. I., Rekni, S. & Nelmes, R. J. (2001). *Phys. Rev. Lett.* **87**, 055501–1–055501–4.
Moseley, P. T. & Seabrook, C. J. (1973). *Acta Cryst.* B**29**, 1170–1171.
Nelmes, R. J., Allan, D. R., McMahon, M. I. & Belmonte, S. A. (1999). *Phys. Rev. Lett.* **83**, 4081–4083.
Otwinowski, Z. & Minor, W. (1997). *Methods in Enzymology*, Vol. 276, pp. 307–326. New York: Academic Press, Inc.
Pearson, W. B. (1972). *The Crystal Chemistry and Physics of Metals and Alloys*. New York: Wiley.
Petricek, V. & Dusek, M. (2001). *The Crystallogaphic Computing System.* Institute of Physics, Academy of Sciences of the Czech Republic, Praha.
Schwarz, U., Grzechnik, A., Syassen, K., Loa, I. & Hanfland, M. (1999). *Phys. Rev. Lett.* **83**, 4085–4088.
Young, D. A. (1991). *Phase Diagrams of the Elements*. Berkely, CA: University of California Press.